

**INTERNATIONAL JOURNAL OF ENGINEERING SCIENCES & RESEARCH
TECHNOLOGY****DEVELOPMENT OF NOVEL CORROSION RESISTANT ELECTROLESS NI-P
COMPOSITE COATINGS FOR PIPELINE STEEL****Lamita Masry¹, George Jarjoura*¹, Zoheir Farhat¹, Eman M. Fayyad², Aboubakr M. Abdullah²,
Mohammad K. Hassan² and Adel Mohamed³**¹Department of Mechanical Engineering, Dalhousie University, Halifax, NS, Canada B3J 2X4²Center for Advanced Materials, Qatar University, P.O. Box 2713, Doha, Qatar³Department of Metallurgical and Materials Engineering, Faculty of Petroleum and Mining
Engineering, Suez University, Box 43721, Suez, Egypt

DOI: 10.5281/zenodo.1189054

ABSTRACT

In order to enhance protective property of electroless Nickel coating, we made electroless Ni-P composite coatings using titanium and Graphene. The corrosion resistance of each coated sample was measured using polarisation methods and electrochemical impedance spectroscopy (EIS) and compared to the Ni-P sample. Their surface morphology and chemical composition were analyzed using scanning electron microscopy (SEM) and energy dispersion spectroscopy (EDS). The objective of this study was to investigate the suitability of applying electroless Ni-P composite coating in the oil and gas industry by characterizing its corrosion behavior. The suitability of applying electroless Ni-P composite coatings in the oil industry was assessed.

I. INTRODUCTION

Carbon steel is the most widely used engineering material and can be used in marine applications, nuclear, chemical processing, and construction equipment. It also has extensive usage in oil industry. Pipelines, made of steel, are a critical infrastructure in oil and gas transportation, they are considered to be the safest and most cost-effective way for transporting large volumes of petroleum products. Oil and gas are transferred by pipelines from excavation to refineries, terminals and markets. However, corrosion of pipeline steel is an increasing problem across the oil and gas industry and results in high costs[1]. Therefore, many surface treatment methods are applied to improve its corrosion resistance and extend its service life. Some of the more common plating technologies are Electroplating, Electroless coating and with minor use there are: Anodizing, carburizing, PVD/CVD, plasma spray coating, to name a few. Among all various surface modification techniques, electroless deposition of nickel-phosphorous (Ni-P) was proved to be the most effective method to modify the physical and chemical properties of the substrates. Moreover, electroless coatings are naturally passive and very resistant to corrosion attack in most environments and extensive range of pH. That made from electroless Nickel-Phosphorus (EN) coating a very efficient method used for protecting steel due to its excellent corrosion, wear and abrasion resistances. It is also known that this technique will form a controllable and uniform deposit on substrate when compared with electroplating, even on parts with complicated shapes[2,3,4,5].

EN coating has a potential use in the oil and gas industry as a protective coating against erosion for the inner surface of pipes. However, corrosion resistance of Ni-P coatings can be improved by adding co-depositing particulate materials in the coating.

The ability to co-deposit particulate substances in a Ni-P coating matrix created a new branch of coatings, namely, Ni-P composite coatings[6,7]. It recently became very useful to endow new features to the EN coatings.

II. EXPERIMENTAL**Sample preparation**

Samples for this study consisted of disks of AISI 1018 steel, 1.5cm in diameter and 6 mm in thickness. AISI 1018 was analysed using inductively coupled plasma mass spectrometry (ICP-MS) and the chemical composition is presented in Table 2.1

Table 2.1. Chemical composition of AISI 1018 in wt. %

Mn	C	S	P	Fe
0.60-0.90	0.15-0.20	0.05 max	0.04 max	Balance

Samples were ground using 240, 320, 400, and 600 silicon carbides (SiC) abrasive papers, then polished using 5, 3 and 1 μm gamma diamond paste. Following polishing samples were cleaned in an ultrasonic cleaner and dried. The purpose of grinding was to clean the surface and remove saw marks. Tap water was necessary while grinding to lubricate and facilitate the interaction between the abrasive paper and the specimen. Polishing was done in purpose to examine the microstructure. After polishing, the surface of the sample seemed like a mirror. It must be well cleaned with water and dried immediately to prevent any corrosion marks. Figure 2.1 shows the aspect of the samples before and after grinding/polishing.



Figure 1. AISI 1018 steel samples before and after grinding/polishing

Pre-treatment

Following ultrasonic cleaning and drying, samples were degreased in an acetone solution for 30s. Degreasing was followed by alkaline cleaning, in a bath consisting of 50 g/L sodium hydroxide, 30 g/L sodium carbonate and 30 g/L sodium phosphate at 80 ± 5 °C for 5 min. Samples were then etched with a 15% aqueous H₂SO₄ solution for 15s. Each step of the process was followed by rinsing the samples in distilled, deionized water. Pre-treatment steps are shown in Figure 2.2.

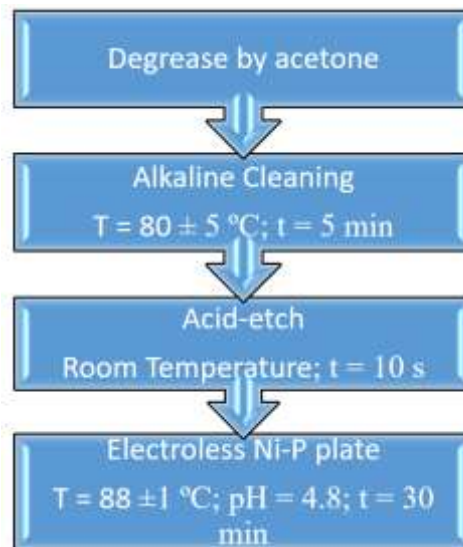


Figure 2.2. Pre-treatment steps

Pre-coating procedure

After pre-treatment, specimens were hung vertically and dropped for a period of 30 mins, at temperature of 89 - 90°C, in 1L of electroless Ni-P solution. The coating solution used in this study was a standard commercial

[Jarjoura * *et al.*, 7(2): March, 2018]
ICTTM Value: 3.00

grade, with nickel sulfate as the main salt and sodium hypophosphite as the reducing agent. This step ensured that a coherent and compact Ni-P coating covered the steel substrate in preparation to the composite coating.

Coating procedure

For composite coating solutions, mixing was done for a period of 30 mins. After getting a homogeneous solution, samples for each type of composite coating (pre-coated with Ni-P) were immersed for different coating periods: 60, 90 and 120 minutes, to vary the coating thickness. Bath conditions for each different coating are given in Table 2.2.

Table 2.2. Bath conditions for the composite coating solutions

Parameter	Ni-P-Ti	Ni-P-Graphene
Temperature (°C)	85-90	85-90
Concentration (g/L)	1	0.3
Magnetic agitation (rpm)	200	200
Surfactant (acetone)	0	Trace

Coating morphology and composition

After plating for the specified times, specimens were removed, cleaned in deionized water and dried in air. In order to check the thickness, distribution and deposition rate; specimens with different coating times were then sectioned using Buehler Isomet 1000 precision saw with diamond blade at a speed of 150 rpm/h. Because the sample is too small, it had to be mounted before grinding and polishing. Epoxy was chosen as cold mounting and had to be heated in oven at 85°C for 3 hours. A Hitachi S-4700 scanning electron microscope (SEM) operating at 10 KV and 15μA, shown in figure 2.3, was used to examine coating morphology and thickness, and an Energy Dispersive Spectrometry (EDS) coupled to the SEM was used to determine the chemical composition and distribution in the coating.



Figure 2.3. Scanning Electron Microscope (SEM)

Corrosion tests/Electrochemical measurements

The corrosion performance of Ni-P, Ni-P Ti and Ni-P-Graphene plating in 3.5 wt. % sodium chloride (NaCl) solution was assessed by linear sweep polarization, cyclic polarization and EIS in a three-electrode electrochemical cell.

The testing cell consisted of:

- A working electrode where the potential is applied
- A reference electrode where the applied potential is measured
- A counter electrode (platinum mesh) to complete the circuit

The test cell is designed to expose 1 cm² of the samples to the saline solution. The reference electrode was maintained at a close distance from the sample using a Luggin Capillary. Figure 2.4 shows the three-electrode cell.

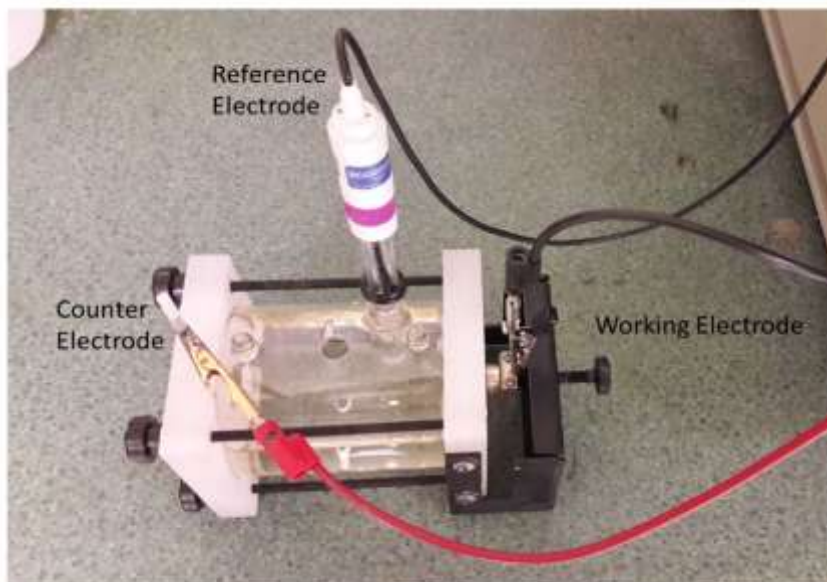


Figure 2.4. The three-electrode cell

Linear sweep polarization (LSP)

In this test, the potentiostat sweeps the working electrode potential at a given scan rate and measures the current. The data obtained from the test are then plotted on an E vs Log (i) plot. The test possesses several advantages:

- It is fast and easy to run
- Inexpensive
- Produces reproducible data with accuracy and precision
- Allows the derivations of several parameters (anodic charge, open circuit potential, rupture potential, passivity range, pitting corrosion) [8]

In the current study, linear sweep polarization tests were done by sweeping the potential from -0.5V (cathodic region) to 1.5V (anodic region) using a scan rate of 0.25mV/s. All the tests were started once steady state was achieved.

The data was then analysed by an electrochemical software, CorrWare, using the Tafel Extrapolation technique. This technique consists of extrapolating the linear areas of the polarization curve to obtain the current density i_{corr} and corrosion potential E_{corr} . After which, i_{corr} is used to calculate the corrosion rate of the sample.

Cyclic polarization (CP)

This test is used to assess the susceptibility of an alloy to localized corrosion (pitting or crevice corrosion). In this test, the potential applied to the test sample under study is ramped at a continuous, often slow, rate relative to a reference electrode using a potentiostat. The voltage is first increased in the anodic or noble direction (forward scan) then reversed at some chosen current or voltage and progresses in the cathodic or active direction (backward or reverse scan). The scan is terminated at another chosen voltage, usually either the corrosion potential or some potential active with respect to the corrosion potential.

In the current study, the cyclic polarization tests were done by scanning the potential starting from -0.5V (cathodic region) to the final potential of -0.5V versus Open Circuit Potential using a scan rate of 0.25mV/s. All tests were started once steady state was achieved.

Data obtained from these tests were used to obtain the pitting potential, corrosion and protection potentials. The corrosion potential is determined from the forward scan peak. The pitting potential is determined from the



forward or ascending portion of the scan where a rapid rise in current occurs. The protection potential is determined from the peak of the reverse scan[9].

Electrochemical Impedance Spectroscopy (EIS)

The principle of this technique is to measure the impedance between the current and the potential at a fixed DC (direct current) potential during a frequency scan with a fixed superimposed AC (alternating current) signal of small amplitude. Data obtained from this test are presented on Nyquist and Bode plots.

In the current work, the impedance measurements were made at a high frequency range by performing the lock-in experiment, followed by a Fast Fourier transform (FFT) experiment, which measures the impedance in the lower frequency range. In the lock-in experiment, the impedance of the sample was measured by imposing a 10 mV AC voltage (sine wave) measuring the AC current and voltage within the lock-in, then calculating the impedance of the coating at a particular frequency. The charge transfer resistance (R_{ct}) and double layer capacitance (C_{dl}) were determined from the corresponding Nyquist plots by fitting the data using Zview software.

III. RESULTS AND DISCUSSION

Coating morphology and composition

Prior to any corrosion testing, coatings on samples were verified to have two layers (the pre-coating and the coating). The thickness, chemical composition and distribution of the elements in the coating were all examined. Smooth, uniform and dense coatings were successfully deposited on the steel substrate. Figure 3.1 and 3.2 show the SEM and EDS for a cross section of respectively titanium and Graphene for 2 hours coating. The chemical compositions of the coatings are shown in Tables 3.1 and 3.2 as can be seen, the surfaces of both coatings exhibit a nodular shape with a typical cauliflower-like morphology in which one big nodule includes many fine ones. The coatings have a uniform distribution of both titanium and Graphene in every part of the coating. The interface between the coating and the steel substrate does not show any defects or cracks at the substrate-coating interface, this demonstrates the good adhesion of the Ni-P-Ti and Ni-P-Graphene coatings. The thicknesses for 2h coatings were estimated to be 70 μm for the titanium coating and 60 μm for the Graphene coating.

All the particles were well incorporated in the Ni-P coating but in different percentages as seen in Table 3.1. The carbon content in the Graphene coating was marked to be higher on surface, which can be attributed to the fact that some Graphene particles were agglomerated during the deposition process.

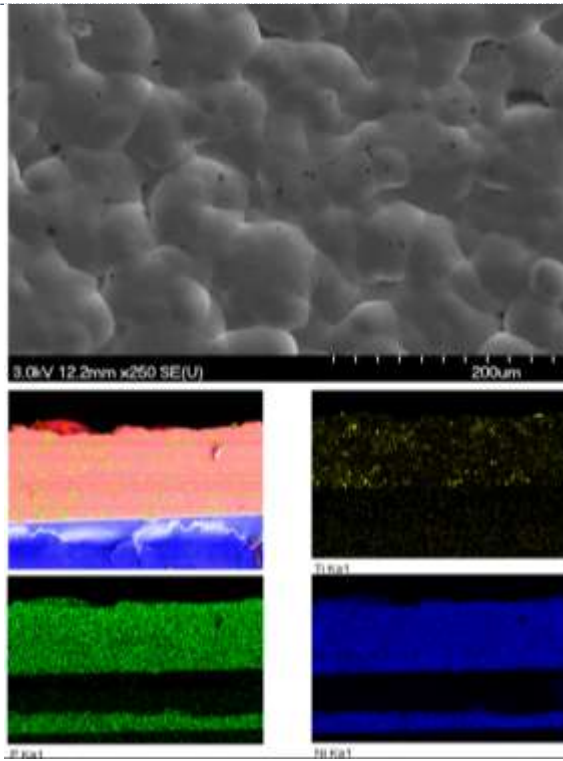


Figure 3. SEM and EDS pictures of Ni-P-Ti coating

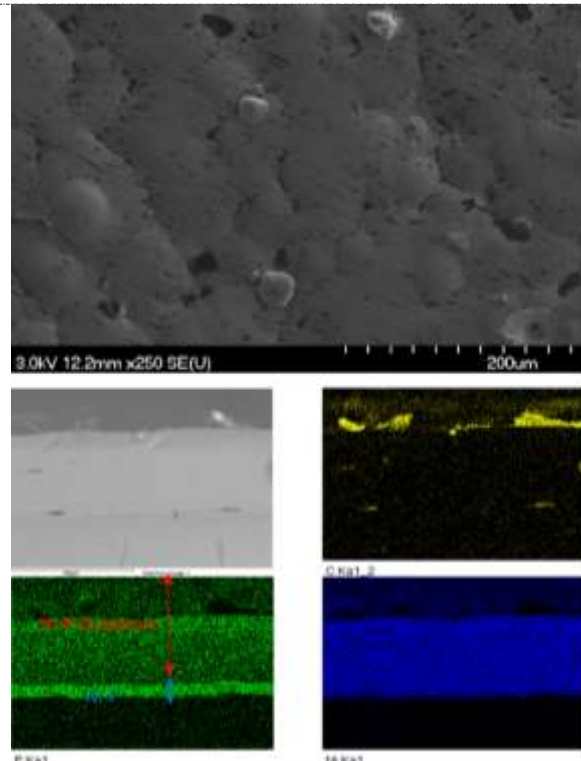


Figure 4. SEM and EDS pictures of Ni-P-Graphene coating

Table 3.3. Chemical composition of Ni-P-Ti sample from cross section

Element	Wt%	At%
Ti	15.21	17.44
P	9.92	17.59
Ni	76.90	71.93

Table 3.4. Chemical composition of Ni-P-Graphene sample from cross section

Element	Wt%	At%
C	4.33	16.86
P	8.14	12.31
Ni	87.04	69.41

Corrosion tests

Linear Sweep Polarization (LSP)

From the potentiodynamic polarisation curves, the corrosion current density i_{corr} and the corrosion potential E_{corr} were extrapolated at the intersection between tangential slopes of the anodic and cathodic curves. E_{corr} gives an idea about the nobility of the coating while i_{corr} gives an idea about the corrosion rate once the corrosion occurs.

Corrosion rate values are given in Table 3.3. Figures 3.3, 3.4 and 3.5 show the LSP curves of the samples with respectively Ni-P, Ni-P-Ti and Ni-P-Graphene coatings (for 120 mins coating time) and the substrate. The corrosion potential (E_{corr}) and corrosion current density (i_{corr}) calculated using Tafel extrapolation on these

[Jarjoura * *et al.*, 7(2): March, 2018]
ICTM Value: 3.00

curves, are given in Table 3.3. All coatings had a more positive corrosion potentials and lower corrosion current density as compared to that of the substrate, which is an indication of more nobility and lower corrosion rate. Compared to the Ni-P coating, it can be seen that both Ni-P-Ti and Ni-P-Graphene coating have lower corrosion current density which indicates better corrosion resistance in saline environments than Ni-P coating. The corrosion potential did not vary too much, that means that the composite does not really affect the coating nobility. The major improvement was in the corrosion rate.

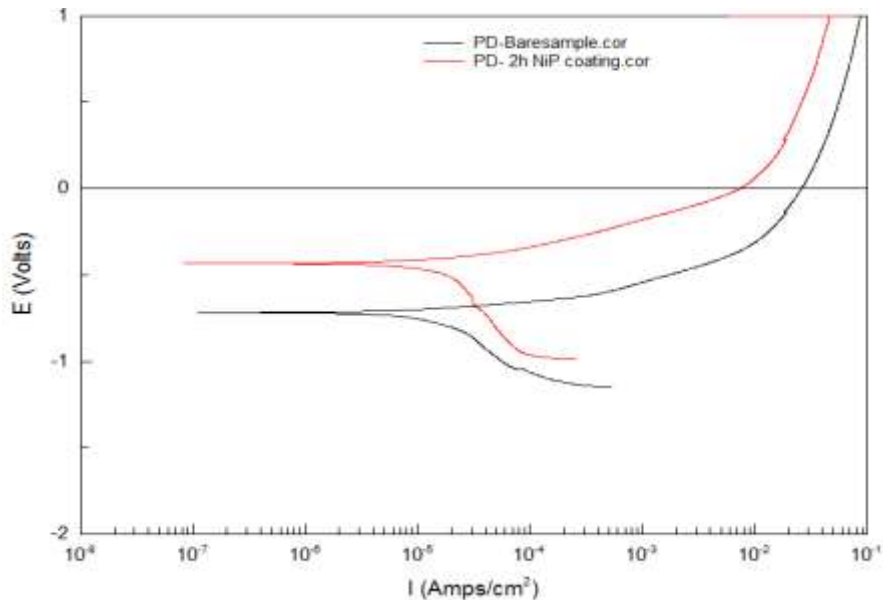


Figure 5. LSP curves of the substrate and the 120 mins Ni-P coating

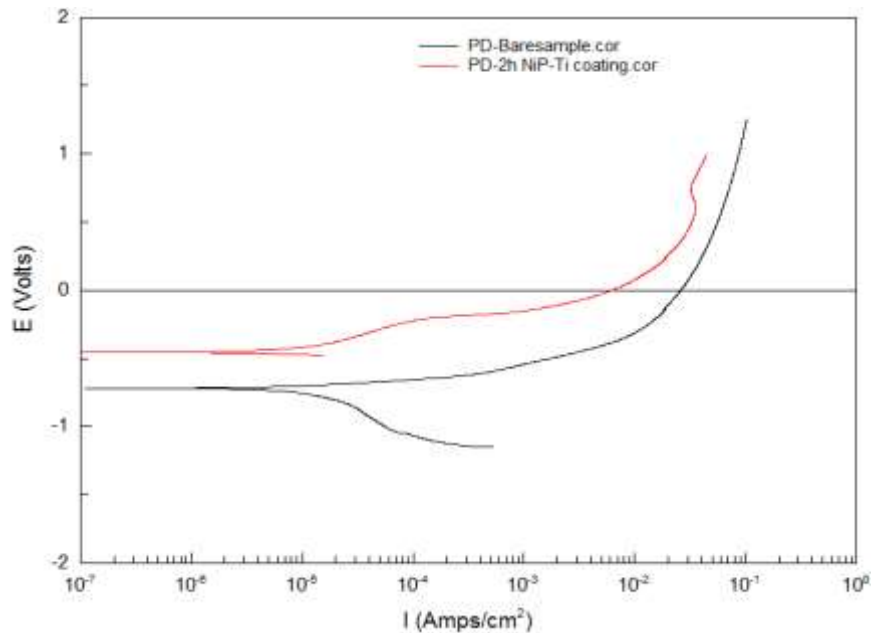


Figure 6. LSP curves of the substrate and the 120 mins Ni-P-Ti coating

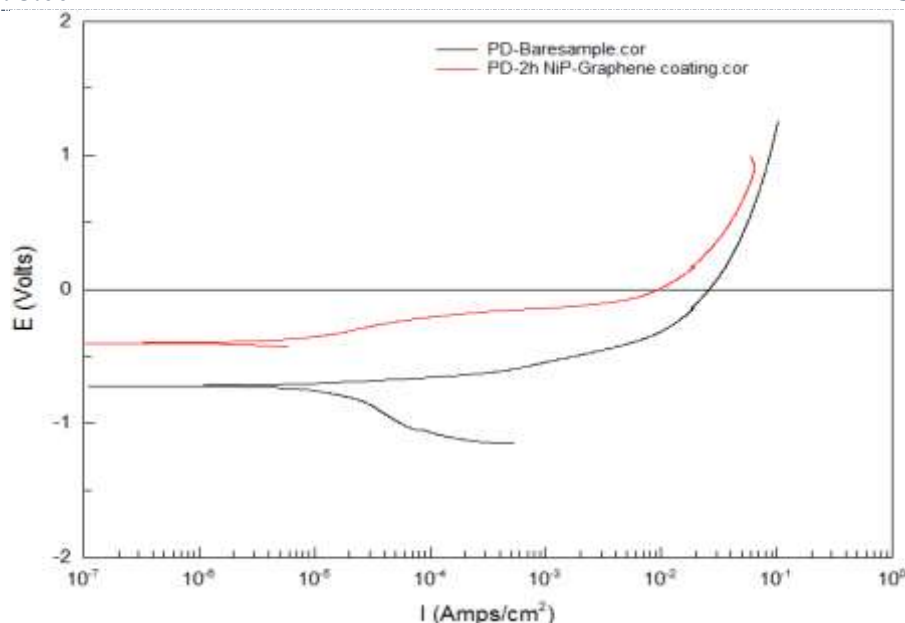


Figure 7. LSP curves of the substrate and the 120 mins Ni-P-Graphene coating

Table 3-5. Electrochemical data from Tafel curve carried out in 3.5% NaCl

Sample	Coating Time (min)	E_{corr} (V)	i_{corr} ($\mu\text{A}/\text{cm}^2$)	CR (mm/yr)
Substrate	-	-0.71	90	1.0362
Ni-P coating	120	-0.43	20	0.2303
Ni-P-Ti coating	120	-0.48	9	0.1036
Ni-P-Graphene coating	120	-0.40	7.5	0.0863

Figure 3.6 shows the corrosion rate (CR) values obtained for each type of coating. The lowest corrosion rate is 0.0863 mm/yr, reached with the Ni-P-Graphene, followed by the Ni-P-Ti composite coating and Ni-P coating. These results indicate that additions of either Graphene or titanium to the Ni-P coating will improve the corrosion resistance in saline environments. This could be due to an easier formation of the passive film in these composite coatings.

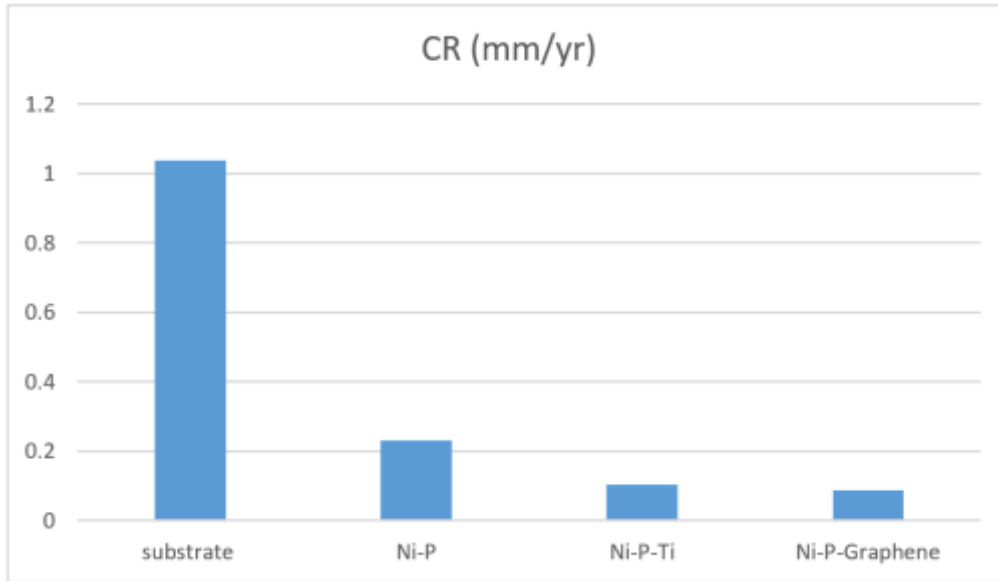


Figure 8. CR of the 3 coatings and the substrate

Cyclic Polarization (CP)

Figures 3.7, 3.8 and 3.9 represent the cyclic polarization curves obtained with respectively samples of Ni-P, Ni-P-Ti and Ni-P-Graphene coatings (coated for 120 minutes). The corrosion potential (E_{corr}), protection potential (E_{prot}) and pitting potential (E_{pit}) obtained from these curves are given in Table 3.4.

The most important parameter to examine is the difference between the corrosion potential and the protection potential, not the values of the potentials themselves. Beyond these two potentials, pitting corrosion starts to take place. Thus, the minor the difference between the corrosion potential and the protection potential, the minor the risk of pitting to appear, the greater the resistance to corrosion will be[33].

The hysteresis refers to a feature of the polarization scan in which the forward and reverse portions of the scan do not overlay each other. The larger the hysteresis loop, the greater the disruption of surface passivity, the greater the difficulty in restoring passivity, and, usually, the greater the risk of localized corrosion.[33].

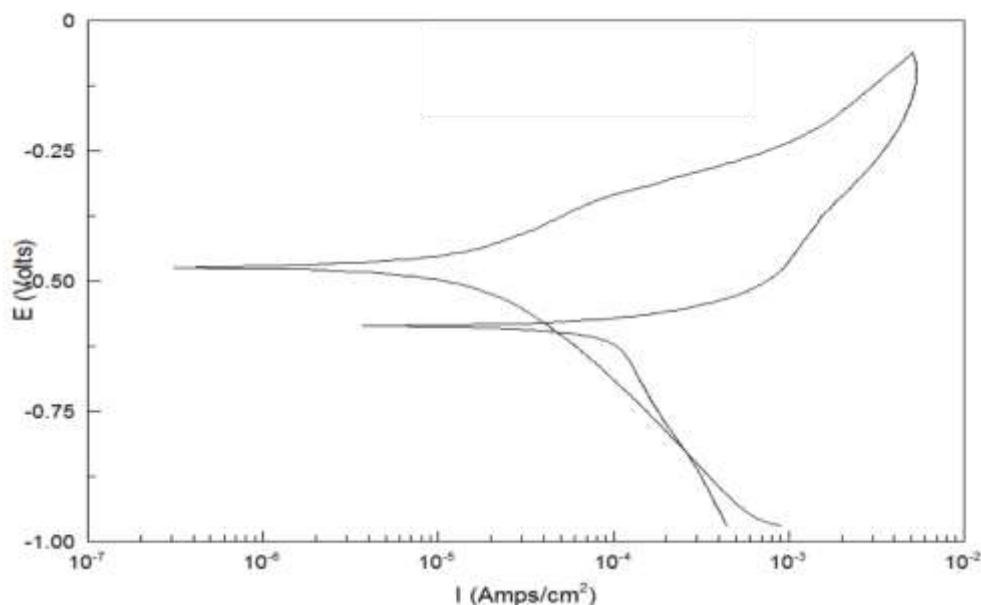


Figure 9. CP curve of 120 mins Ni-P coating

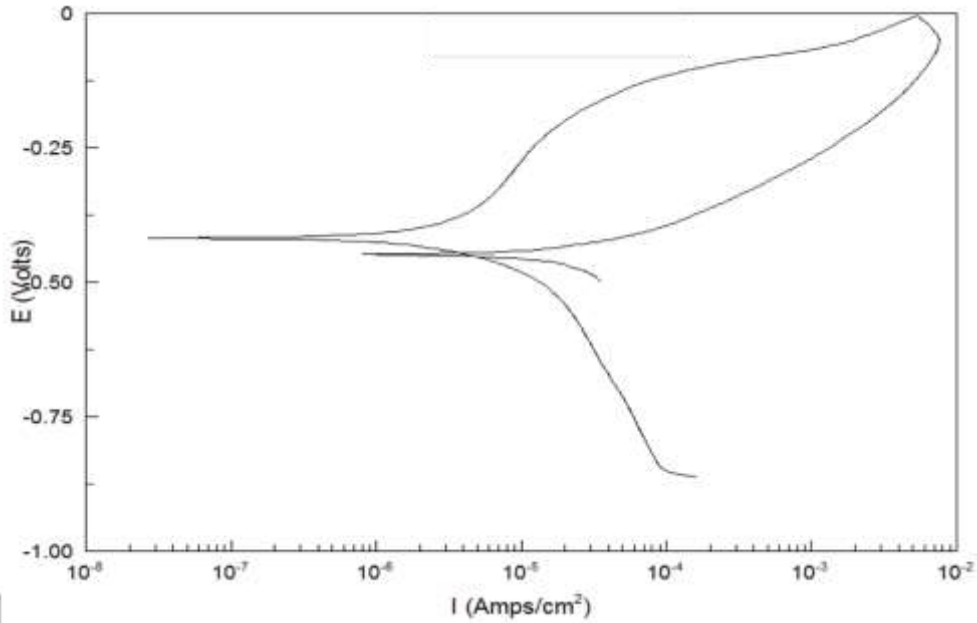


Figure 10. CP curve of 120 mins Ni-P-Ti coating

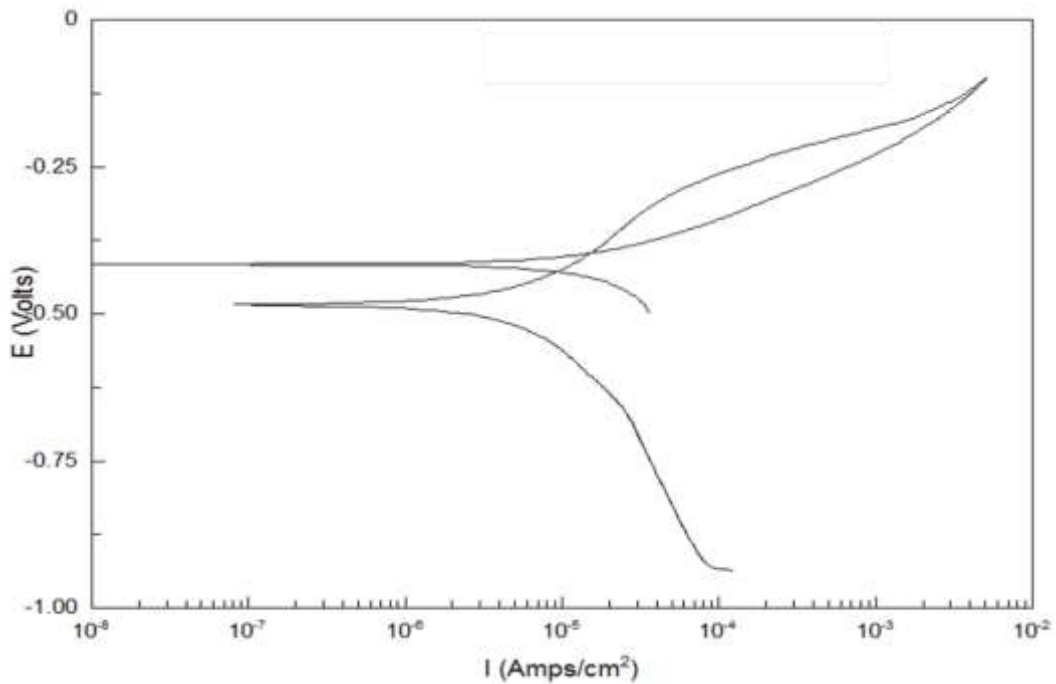


Figure 11. CP curve of 120 mins Ni-P-Graphene coating

Table 3.6: Results of the cyclic polarization test

Type of coating	Time of coating	$E_{corr}(V)$	$E_{prot}(V)$	$E_{pit}(V)$
Ni-P	2h	-0.474	-0.586	-0.201
Ni-P-Ti	2h	-0.419	-0.448	-0.111
Ni-P-Graphene	2h	-0.484	-0.415	-0.253

[Jarjoura * *et al.*, 7(2): March, 2018]
ICTM Value: 3.00

It can be seen from these results that Ni-P coating has the most tendency to pitting corrosion since it has the largest difference between the corrosion potential and the protection potential, and the largest hysteresis loop. Ni-P-Ti coating had the minor difference between the corrosion potential and the protection potential but the hysteresis loop was very large. Whereas for Graphene, the hysteresis loop has the best shape compared to Ni-P and Ni-P-Ti, plus, the difference between the corrosion potential and the protection potential was not very large. So, it can be concluded from these results that Graphene was the best to improve the corrosion resistance of the coating since it has the best resistance to pitting.

Electrochemical Impedance Spectroscopy (EIS)

Figure 3.10 shows the EIS spectra of Bode plots and the corresponding phase angle plots; these were obtained at open circuit potential for the Ni-P, Ni-P-Ti and Ni-P-Graphene coatings immersed in a 3.5 wt% NaCl solution at room temperature. It is well known that the larger value of R_p at low frequencies corresponds to better corrosion protection properties of the coating. Inspection of values of R_p for all three coatings shows that R_p for Ni-P-Ti and Ni-P-Graphene are considerably higher than that for Ni-P, indicating a significant improvement of the corrosion protection with the addition of Ti and Graphene particulates. Generally, for a Ni-based coating, when the nickel starts to dissolve in the corrosive media, the phosphorus starts to react with water to form a film of adsorbed hypophosphite anions, preventing further hydration of the nickel. Consequently, the corrosion resistance of the coating is increased. Moreover, the Ni-P-Ti and Ni-P-Graphene composite coatings offer extra corrosion protection ability compared to that of the Ni-P coating as seen from the values of R_p . This finding indicates the strong protective ability of the Ti and Graphene nanoparticles that enhance the polarization resistance of the Ni-P coating in 3.5 wt% NaCl solution reaching its maximum value of 48 k Ω , as shown in Table 3.5. This can be attributed, as mentioned above, to the nanoparticles' uniform distribution throughout the coating and the boundaries blocking the defects and dislocations in the Ni-P coating, inhibiting the diffusion of the chloride ions to the substrate and enhancing the corrosion resistance.

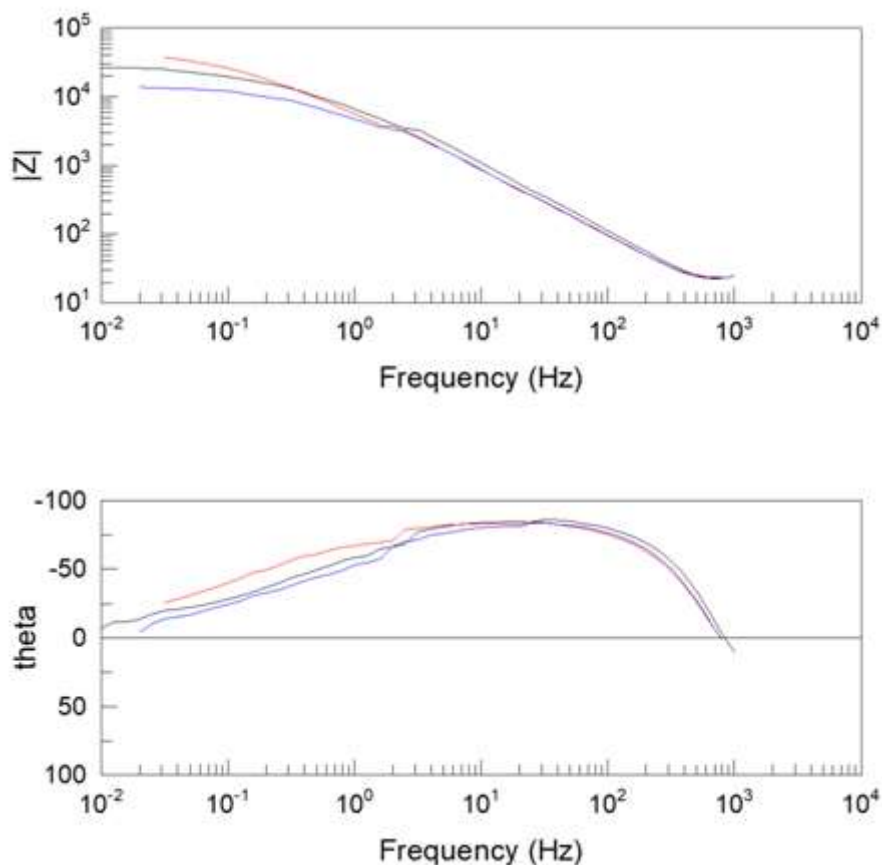


Figure 3-10. Bode and phase angle plots of Ni-P, Ni-P-Ti and Ni-P-Graphene coatings

[Jarjoura * *et al.*, 7(2): March, 2018]
ICTM Value: 3.00

To account for the corrosion behaviour of the coatings at their respective open circuit potentials, an equivalent circuit model given in Figure 3.11 has been utilized to simulate the metal/solution interface and to analyse the plots.

The equivalent circuit includes the solution resistance (R_s), the high frequency time constant, which is represented by the coating capacitance and the pore resistance (C_{coat} , R_{po}) and the low frequency time constant, which is represented constant phase element of the double layer and the polarization resistance (CPE_{dl} , R_p). The best fitted electrochemical parameters for the equivalent circuits representing the coatings are listed in Tables 3.5, 3.6 and 3.7.

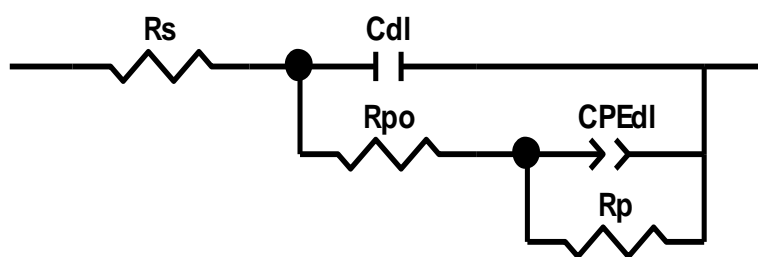


Figure 12. Equivalent circuit of the Ni-P, Ni-P-Ti and Ni-P-Graphene coatings

As it can be concluded, increased polarization resistance is related to the presence of the Ti and Graphene nanoparticles. Moreover, the composite coatings have lower values of the double layer CPEs compared to the one for the NiP coating. This increase gives rise to the superior protection efficiency of the composite coatings.

Table 3.7: Electrochemical parameters of Ni-P coating

Element	Value
R_s	22.7
C_{coat}	1.891E-05
R_{po}	755.2
CPE_{dl-T}	4.5327E-05
CPE_{dl-P}	0.6751
R_p	17854

Table 3.8. Electrochemical parameters of Ni-P-Ti coating

Element	Value
R_s	21.48
C_{coat}	1.516E-05
R_{po}	991.9
CPE_{dl-T}	3.388E-05
CPE_{dl-P}	0.69931
R_p	30937

Table 3.9. Electrochemical parameters of Ni-P-Graphene coating

Element	Value
R_s	24.2
C_{coat}	1.8789E-05
R_{po}	217.8
CPE_{dl-T}	3.8083E-05
CPE_{dl-P}	0.79451
R_p	48231

IV. CONCLUSIONS

The following conclusions can be drawn from the this work:

- The composite coatings were successfully deposited on the steel substrate.
- Titanium and Graphene particles were successfully dispersed in the coatings, with some agglomeration occurring in the Graphene case.
- All coatings showed adhesion to the substrate as well as excellent compaction.
- From the Linear polarization test it was concluded that the addition of titanium and Graphene resulted in lowering the corrosion current densities, consequently lowering the corrosion rates without significantly changing the coatings' nobility. The lowest corrosion rate was reached with the Ni-P-Graphene coating.
- The cyclic polarization test showed that adding Graphene particles resulted in the best corrosion resistance improvement against pitting corrosion.
- The EIS results obtained proved from the values of R_p that the Ni-P-Ti and Ni-P-Graphene composite coatings offer extra corrosion protection ability compared to that of the Ni-P coating.

V. ACKNOWLEDGMENTS

This work was supported by NPRP grant # NPRP8-1212-2-499 from the Qatar National Research Fund (a member of Qatar Foundation)

VI. REFERENCES

- [1] Xiu-qing, X., et al., The corrosion behavior of electroless Ni-P coating in Cl⁻/H₂S environment. *Applied Surface Science*, 2012. 258(22): p. 8802-8806.
- [2] Luo, H., et al., Development of electroless Ni-P/nano-WC composite coatings and investigation on its properties. *Surface and Coatings Technology*, 2015. 277: p. 99-106.
- [3] Taheri, R., Evaluation of electroless nickel-phosphorus (EN) coatings. University of Saskatchewan Saskatoon, 2002.
- [4] Mallory, G.O. and J.B. Hajdu, *Electroless plating: fundamentals and applications*. 1990: William Andrew.
- [5] Deng, H. and P. Moller, Effect of the substrate surface morphology on the porosity of electroless nickel coatings. *Transactions of the IMF*, 1993. 71(4): p. 142-148.
- [6] Sudagar, J., J. Lian, and W. Sha, Electroless nickel, alloy, composite and nano coatings—A critical review. *Journal of Alloys and Compounds*, 2013. 571: p. 183-204.
- [7] Barker, D., Electroless deposition of metals. *Transactions of the IMF*, 1993. 71(3): p. 121-124.
- [8] HOLLAND, R.I., Use of potentiodynamic polarization technique for corrosion testing of dental alloys. *European Journal of Oral Sciences*, 1991. 99(1): p. 75-85.
- [9] Silverman, D.C., Tutorial on cyclic potentiodynamic polarization technique. 1998, NACE International, Houston, TX (United States)..

CITE AN ARTICLE

Masry, L., Jarjoura, G., Farhat, Z., Fayyad, E. M., Abdullah, A. M., Hassan, M. K., & Mohamed, A. (n.d.). DEVELOPMENT OF NOVEL CORROSION RESISTANT ELECTROLESS NI-P COMPOSITE COATINGS FOR PIPELINE STEEL. *INTERNATIONAL JOURNAL OF ENGINEERING SCIENCES & RESEARCH TECHNOLOGY*, 7(3), 122-134.